

Article

Bi-Objective Optimization of Vessel Speed and Route for Sustainable Coastal Shipping under the Regulations of Emission Control Areas

Yuzhe Zhao ^{1,*}, Yujun Fan ¹ , Jingmiao Zhou ² and Haibo Kuang ¹

¹ Collaborative Innovation Center for Transport Studies, Dalian Maritime University, Dalian 116026, China; yujunfan@dmlu.edu.cn (Y.F.); 18698606670@163.com (H.K.)

² Business School, Dalian University of Foreign Languages, Dalian 116044, China; zhoujingmiao123@126.com

* Correspondence: zhaoyuzhe@126.com

Received: 29 July 2019; Accepted: 5 November 2019; Published: 8 November 2019



Abstract: To comply with the regulations of emission control areas (ECAs), most operators have to switch to low-sulfur fuels inside the ECAs. Besides, a low-carbon objective is essential for long-term environmental protection; thus, is regarded as important as making profit. Therefore, the operators start making speed and route decisions under the two objectives of minimizing carbon emissions and maximizing profit. Drawing on existing methods, this paper formulates the profit and carbon emissions in sustainable coastal shipping, investigates the speed and route principles, and determines the best tradeoff between profit and carbon emissions. It is found that vessel speed should be set between emissions-optimum speed and profit-optimum speed, and the route must be selected in light of the speed decision. Next, the optimal choices of speed and route were examined under different scenarios and vessel types. The results show that the operation measures and objectives depend greatly on fuel price, vessel load, and vessel parameters. The operator should speed up the vessel if he/she wants to make more profit or if the scenario is favorable for profit making; e.g., low fuel price and high vessel load (LFHL). Large vessels should pursue more profit under LFHL conditions, without having to sail further outside the ECA. But this rule does not apply to small vessels. In addition, the operator should slow down the vessel inside the ECA and sail further, outside the ECA, with the growth in the price spread between marine gas oil (MGO) and heavy fuel oil (HFO), especially at a low HFO price. The research findings help operators to design operational measures that best suit the limit on sulfur content in fuel and the situation of the shipping market.

Keywords: emission control areas (ECAs); vessel speed; vessel route; sustainable coastal shipping; carbon emissions; bi-objective optimization

1. Introduction

The past few decades have witnessed a considerable growth in the emissions of noxious gases and greenhouse gases (GHGs) in maritime transport, causing various negative impacts on human health and the environment [1]. Coastal emissions occupy a large proportion in global shipping emissions, almost 70% of which occur within 400 km (216 nautical miles) of the coast [2]. Therefore, sustainable coastal shipping is an effective and inevitable way to address the issues derived from shipping emissions [3]. Generally, sustainable coastal shipping measures can be divided into two aspects corresponding to controlling noxious emissions and reducing GHGs.

1.1. Control of Noxious Emissions

To mitigate the growing noxious gases emissions, the International Maritime Organization (IMO) has designated several emission control areas (ECAs) to limit the sulfur content of vessel fuel, including

the Baltic Sea, the North Sea, the North American coasts, and the US Caribbean coasts. Similarly, the Ministry of Transport of China defined the Chinese coast as a domestic ECA, which came into force in 2019. Currently, the limit on sulfur content within in the Chinese ECA is 0.5%, while the global sulfur limit outside the ECA is 3.5%. An even more stringent sulfur limit of 0.1% is under consideration by the Chinese authorities and may take effect in 2025. In addition, the global sulfur limit will be reduced to 0.5% in 2020.

To comply with the limit on sulfur content, vessel operators must either use pricier liquified natural gas (LNG) and low-sulfur fuels like marine gas oil (MGO), or invest in abatement technologies like scrubber systems, which require relatively high capital costs [4]. Currently, the most widely adopted method is switching to low-sulfur fuels [5,6]. The limit on sulfur content directly pushes up the cost for shipping operations inside the ECAs, especially along the coasts. Many vessel operators are forced to sail longer distances rather than pass through the ECAs [7]. Besides, the coastal shipping sector may be outcompeted by land-based transport modes that are not directly affected by the strict sulfur regulations, leading to the decline of vessel loads [8]. This poses a serious threat to maritime transport in China, where 59.7% of the shipping throughput is realized by bulk carriers and containerships in the coastal shipping sector. Against this backdrop, it is imperative to enhance the competitiveness of the coastal shipping sector through proper decision-making, such as optimizing speed and route [9,10]. It should be noted that controlling noxious emissions are requirements from the ECA regulations, and thus, are actually considered a policy constraint, rather than an objective for operators when making decisions of speed and route.

1.2. Reduction of GHG Emissions

In contrast with the control of noxious emissions, although GHGs (mostly carbon emissions) are not controlled by the ECA regulations as of yet, the operators have positively started taking into account the objective of reducing carbon emissions in the phase of decision-making. For example, the Maersk Line promised to slash their carbon emissions from shipping to zero [11]. The survey recorded in [12] also shows that some operators volunteer to reduce carbon emissions.

This trend of reducing carbon emissions was mainly encouraged by the preferences of governments, shippers, and other stakeholders [13]. Maritime transport contributes greatly to carbon emissions [14,15]. If no action is taken, maritime carbon emissions will grow by 50%–250% in 2050, pushing up the temperature globally [16]. Therefore, increasingly concerned about global warming, governments and the public expect the shipping sector to reduce carbon emissions. For instance, China, in order to reflect the commitment of a responsible power, has proposed that the carbon emissions per unit of gross domestic product in 2030 will be reduced by 60% to 65% compared to 2005. Under the pressure of the government, various industries, including the shipping sector, have set more sustainable objectives. Besides, existing studies have demonstrated that continuous efforts targeted at protecting the environment are favorable to increasing long-term business performance [17,18]. Many shippers and forwarders look forward to sustainable shipping, which may further stimulate the operators to set low carbon objectives [19]. Furthermore, optimizing operational measures of speed and route is a much cheaper way compared with retrofitting vessels to combust low-carbon fuels, such as biofuel.

Summing up, for the operator pursuing sustainable development, the decision-making on speed and route is essentially a tradeoff between the maximal profit and the minimal carbon emissions, while switching to low-sulfur fuels within the ECA to comply to the regulations [20,21].

This paper mainly tackles two questions: Do the level of attention paid to carbon emissions affects the decisions on optimal speed and route change for vessels that switch to low-sulfur fuels under ECA regulations, and if so how? What are the impacts of these decisions on the coastal shipping sector? The authors also explored how fuel price, vessel load, and vessel size affect the sustainable operations of coastal shipping.

There are three main contributions of this research: the existing methods were integrated to compute profit and fuel consumption; several important principles of sustainable shipping operations were given under different objectives, such as the Pareto speed interval, as well as the impacts of

rerouting outside the ECAs; the sustainable shipping operations of vessels with different sizes sailing along coastal China under different scenarios of fuel price and vessel load were examined empirically.

The remainder of this paper is organized as follows: Section 2 reviews the existing studies on the ECA regulations and sustainable operation objectives; Section 3 introduces the method to compute profit and carbon emissions; Section 4 verifies the proposed method through a case study; Section 5 puts forward the research conclusions.

2. Literature Review

2.1. The ECA Regulations and Their Impacts

The ECA regulations require the operator to switch to expensive low-sulfur fuels, and thus have great side effects on many aspects of shipping operations; namely, speed and route [22–24].

Concerning speed, vessel operators may sail at a lower speed inside the ECAs to compensate for the extra cost needed to comply with ECA regulations. Fagerholt and Psaraftis [25] optimized the vessel speed in and out of ECAs based on the Ronen's model [26], and solved the ECA reroute problem by optimizing the point that a vessel crosses the ECA boundary. Similarly, Doudnikoff and Lacoste [27] analyzed the difference between vessel speeds inside and outside of the ECAs. Zis, et al. [28] also demonstrated that the differentiated sailing speeds inside and outside the ECAs, which may further lead to additional carbon emissions per journey. However, some recent studies argue that the strict limit on sulfur content in fuel does not necessarily affect the vessel speed [29]. The studies above ignored how operation objectives affect the impacts on the speed within ECAs. In fact, Lindstad, et al. [14] found that vessel operators make different speed decisions under different objectives. This finding was introduced to study the ECA case in our research.

It is generally agreed that the ECA regulations affect the vessel route. Fagerholt, et al. [9] discovered that vessel operators tend to choose the routes outside the ECAs, despite their longer distances. On this basis, Zhen, et al. [30] analyzed the impacts of the ECAs on the routes of cruise ships. Chen, et al. [31] also suggested that vessels may reroute to avoid sailing in the ECAs. Drawing on the literature, this paper considers that route decisions are influenced by fuel price, vessel load, and sustainable operation objectives.

Besides speed and route, the literature also explored other impacts of ECA regulations. Patricksson and Erikstad [32] analyzed the choices of abatement technology for the shipping companies considering the uncertainty of fuel price; the results found the dual fuel engine and gas engine that can combust liquid natural gas (LNG) has a cost advantage with a time horizon of about 20 years. However, the LNG-fueled vessels make up a very small market share currently. This paper only focused on the operational optimization for the most widely-adopted compliance; i.e., fuel switching. Bergqvist, et al. [33] and Zis and Psaraftis [34] show that the ECA regulations in Europe may increase the freight rate, and thus stimulate the redistribution of cargo flow with land-based alternatives; i.e., modal shift. The possible impact of modal shift was considered and used to set different scenarios in this paper. Our case study analyzed the operational measures under scenarios of different vessel loads and fuel prices.

2.2. Sustainable Operation Objectives

In recent years, shipping operation problems considering environmental impacts have occupied an increasing proportion in the literature [35]. The related literature is often based on single-objective optimization. Corbett, et al. [36] calculated the carbon emissions based on the results of a single-objective, profit maximization model. Kim, et al. [37] set carbon taxation as a constraint of the fuel-cost minimization model. Wen, et al. [38] proposed a cost minimizing model and an alternative, single-objective optimization model, including minimizing trip duration and minimizing emissions.

Besides single-objective optimization, many scholars also investigated the different objectives in sustainable shipping operations with the aim to strike a balance between profit and environment. For instance, Psaraftis and Kontovas [39] explored the effects of various maritime policies on carbon emissions, and attempted to eliminate the environmental impacts by reducing the steaming speed,

changing the number of vessels in the fleet, and using in-transit inventory holdings. Lindstad, et al. [14] analyzed the impacts of speed reduction on cost and carbon emissions, and demonstrated that speed reduction alone can lower carbon emissions with zero abatement costs. Wong, et al. [40] proposed a utility function to strike the balance between fuel cost, carbon emissions, and trip duration. Under the constraints of sensitive demand and ECA regulations, Cheaitou and Cariou [41] developed a multi-objective optimization (MOO) framework to optimize the vessel speed of liner shipping, including different objective functions like profit, carbon emissions, and sulfur oxide emissions. Mansouri, et al. [42] summed up the studies on environmental sustainability, decision support systems, and multi-objective optimization in maritime shipping.

The studies above demonstrate the importance of taking different objectives into account. In this paper, the bi-objective optimization method of Cheaitou and Cariou [41] is extended under multiple scenarios, and adopted to optimize the decisions on speed and route.

3. Methods

This section aims to determine the profit and carbon emissions for vessels sailing partially inside an ECA. The following hypotheses were put forward before modelling: (1) Both the main engine and auxiliary engine use the MGO when a vessel sails inside the ECA; the main engine uses heavy fuel oil (HFO) when the vessel sails outside the ECA, while the auxiliary engine continues to use the MGO [25,27]; (2) extreme weather and unexpected accidents are not worth considering; (3) The vessel speed remains above a lower limit (V) constrained by the charter contract to avoid delivery delay and below an upper limit (\bar{V}) related to the maximum continuous rating of the engine. The input parameters and decision variables are defined in Table 1.

Table 1. A list of the notations.

Input Parameters:	
A	Lightship weight, ton
C	Cost per ton-nautical-mile, USD
C_{fe}	Fuel cost inside the ECA, USD
C_{fn}	Fuel cost outside the ECA, USD
C_{fp}	Fuel cost in ports
C_{td}	Daily cost, time charter equivalent (TCE)
E	Carbon emissions per ton-nautical-mile, ton
EL^A	Load factor of the auxiliary engine, %
EL^M	Load factor of the main engine, %
e_{mgo}	Carbon emissions factor of the MGO
e_{hfo}	Carbon emissions factor of the HFO
f^A	Daily fuel consumption of the auxiliary engine, ton/day
f^M	Daily fuel consumption of the main engine, ton/day
f^M	Daily fuel consumption of the main engine at the design speed, ton/day
f_{fe}^M	Daily fuel consumption of the main engine inside the ECA, ton/day
f_{fn}^M	Daily fuel consumption of the main engine outside the ECA, ton/day
F_{mgo}	MGO consumption, ton
F_{hfo}	HFO consumption, ton
L	Distance of the voyage, nautical mile
P	Profit per ton-nautical-mile, USD
P_{mgo}	MGO bunker price
P_{hfo}	HFO bunker price
PS^A	Auxiliary engine power, kW
PS^M	Main engine power, kW
R	The total revenue per voyage, USD
$SFOC^A$	The amount of fuel used per kWh of the auxiliary engine, g/kWh
$SFOC^M$	The amount of fuel used per kWh of the main engine, g/kWh
T_e	The sailing time inside ECA, day
T_n	The sailing time outside ECA, day
T_p	The time spent in ports, day
V	Design speed, knot
W	Vessel load, ton
μ_o	The loading efficiency in the origin port, ton/h
μ_d	The loading efficiency in the destination port, ton/h
λ_o	The cargo handling charge in the origin port, USD/ton
λ_d	The cargo handling charge in the destination port, USD/ton
Decision Variables:	
v_e	The speed inside the ECA, knot
v_n	The speed outside the ECA, knot
X	The ratio of the distance outside the ECA to the distance of the voyage (the distance ratio)

3.1. Formulations of Fuel Consumption

In the previous research that deals with vessel speed [26], the daily fuel consumption of the main engine was often assumed to be a cubic function of vessel speed:

$$f^M = f^{M*} \left(\frac{v}{V} \right)^3 \quad (1)$$

where v is the vessel speed. Considering both vessel speed and load, the modified admiralty coefficient formula can approximate fuel consumption more realistically [43–45]:

$$f^M = Gv^n(A + W)^{\frac{2}{3}} \quad (2)$$

where G and n are two constants dependent on vessel features (e.g., $G > 0$ and $n \geq 3$). As mentioned in Psaraftis and Kontovas [44], $n = 3$ is a good approximation for bulk carriers. Wang and Meng [46] shows that $n = 3$ can also be a good approximation for containerships if not enough data are available for more accurate calibration.

The result of the cubic function (Equation (1)) may seriously under or overestimate reality. After all, a vessel sailing at a given speed needs to overcome different levels of resistance when it is empty, half-loaded, or fully-loaded. The resistance level determines the fuel consumption of the main engine. If vessel load is neglected ($W = 0$), however, Equation (1) can approximate fuel consumption realistically. Thus, the fuel consumption of the main engine in an empty vessel can be computed by either Equation (1) or (2). The value of G in function Equation (2) can be approximated by:

$$G = \frac{f^{M*}}{V^3 A^{\frac{2}{3}}} \quad (3)$$

Inspired by Cariou and Cheaitou [47] and Doudnikoff and Lacoste [27], the daily fuel consumption of the main engine at the design speed can be expressed as:

$$f^{M*} = (SFOC^{MEL^M PS^M}) \frac{24}{10^6} \quad (4)$$

Combining Equations (2), (3), and (4), the daily fuel consumption of the main engine can be finalized as:

$$f^M = (SFOC^{MEL^M PS^M}) \left(\frac{v}{V} \right)^3 \left(1 + \frac{W}{A} \right)^{\frac{2}{3}} \frac{24}{10^6} \quad (5)$$

Equation (5) gives a more precise result than cubic Equation (1). The vessel parameters in Equation (5) can be directly obtained from vessel specifications.

The auxiliary engine supplies the auxiliary power needed to generate electricity on board. Its fuel consumption is independent of vessel speed. Therefore, the daily fuel consumption of the auxiliary engine can be expressed as:

$$f^A = (SFOC^A EL^A PS^A) \frac{24}{10^6} \quad (6)$$

3.2. Formulations of Time

The sailing time inside ECA, the sailing time outside ECA, and the time spent in ports can be computed, respectively, by:

$$T_e = \frac{(1 - X)L}{24v_e} \quad (7)$$

$$T_n = \frac{XL}{24v_n} \quad (8)$$

$$T_p = \frac{W}{24} \left(\frac{1}{\mu_0} + \frac{1}{\mu_d} \right) \quad (9)$$

3.3. Formulations of Costs, Profit, and Carbon Emissions

The fuel costs are the product of time, daily fuel consumption, and fuel price. The fuel costs inside and outside the ECA can be computed, respectively, by:

$$C_{fe} = T_e P_{mgo} (f_{v_e}^M + f^A) \quad (10)$$

$$C_{fn} = T_n (P_{hfo} f_{v_n}^M + P_{mgo} f^A) \quad (11)$$

The fuel cost in ports was considered to make the cost calculation more realistic. This cost can be calculated by:

$$C_{fp} = P_{mgo} T_p f^A \quad (12)$$

The cost per ton-nautical-mile, C , consisting of fuel costs, cargo handling charges, and the daily cost in TCE (i.e., the financial items, depreciation, and operating cost), can be described as:

$$C = \frac{1}{WL} ((C_{fe} + C_{fn} + C_{fp}) + W(\lambda_O + \lambda_d) + C_{td}(T_e + T_p + T_n)) \quad (13)$$

where the first term $1/WL$ converts the total cost per voyage to the cost per ton-nautical-mile; the second term is the cost of bunker fuel; the third term is the cargo handling charge; the last term is the daily cost in TCE.

The profit per ton-nautical-mile can be obtained by subtracting the cost per ton-nautical-mile from the revenue per ton-nautical-mile:

$$P = \frac{R}{WL} - C \quad (14)$$

The MGO consumption and HFO consumption can be computed, respectively, by:

$$F_{mgo} = T_e (f_{v_e}^M + f^A) + T_n f^A + T_p f^A \quad (15)$$

$$F_{hfo} = T_n f_{v_n}^M \quad (16)$$

As reported by the IMO [16], the carbon emission per ton-nautical-mile can be determined by:

$$E = \frac{1}{WL} (e_{mgo} F_{mgo} + e_{hfo} F_{hfo}) \quad (17)$$

4. Case Study

The formulations in the previous section were applied to determine the vessel speed and route in an actual case. A bi-objective optimization model was set up to optimize the speed and route for different objectives and scenarios. The optimal results were obtained for different vessel types sailing along coastal China. The coastal shipping sector in China was selected as the target, due to its importance and the great challenges it is faced with.

4.1. Data Sources

In this section, the profit and carbon emissions of an actual vessel are computed based on the abovementioned formulations. The vessel, operated by Trawind Shipping Logistics, transports coal from Dalian to Guangzhou [48].

The main parameters of the vessel (Table 2) were obtained directly from Trawind. However, the operator kept the total revenue per voyage, R , as confidential information. The HFO price and MGO price were set to 440 USD/ton and 720 USD/ton, respectively, according to the 2018 fuel prices on Bunkerworld.com [49]. The carbon emission factors of the HFO and the MGO were, respectively, 3.206

and 3.114 [16]. The cargo handling charges in Dalian and Guangzhou were both 4.35 USD/ton, as mentioned on dlport.cn [50] and gzpgroup.com [51]. The loading efficiencies in Dalian and Guangzhou were, respectively, 3600 and 3000 ton/h [50,51].

Table 2. The main parameters of the vessel.

Parameters	Value
Cargo capacity	57,025 dwt
Lightship weight (A)	10,900 tons
Main engine power (PS^M)	9480 kW
Auxiliary engine power (PS^A)	2160 kW
Load factor of the main engine (EL^M)	80%
Load factor of the auxiliary engine (EL^A)	50%
The amount of fuel used per kWh of the main engine ($SFOC^M$)	165 g/kWh
The amount of fuel used per kWh of the auxiliary engine ($SFOC^A$)	225 g/kWh
Design speed (V)	14.2 knots

As of 1 January 2019, a coastal ECA extending 12 nautical miles from the baseline of Chinese territorial sea officially took effect. Any vessel sailing inside the ECA is required to use fuels with a sulfur content no greater than 0.5%. The new sulfur limit forced shipping companies to save costs by rerouting. As shown in Figure 1, Trawind can select from 16 alternative routes, whose distance ratios (X) vary from 0.256 to 0.867. The regression relationship between the total distance and the value of X can be expressed as $L = 194.5X + 1248.9$ ($R^2 = 0.9909$).



Figure 1. Map of the emission control area (ECA) and possible routes.

4.2. Decisions Analysis

4.2.1. Speed Decisions

Figure 2 presents the effects of speed decisions on profit and carbon emissions per million ton-nautical-mile. The left part of the figure shows the variations in profit and carbon emissions with vessel speeds inside the ECA (v_e), when the speed outside the ECA (v_n) was fixed at 8 knots. The right part shows the variations in profit and carbon emissions with v_n , when v_e was fixed at 8 knots.

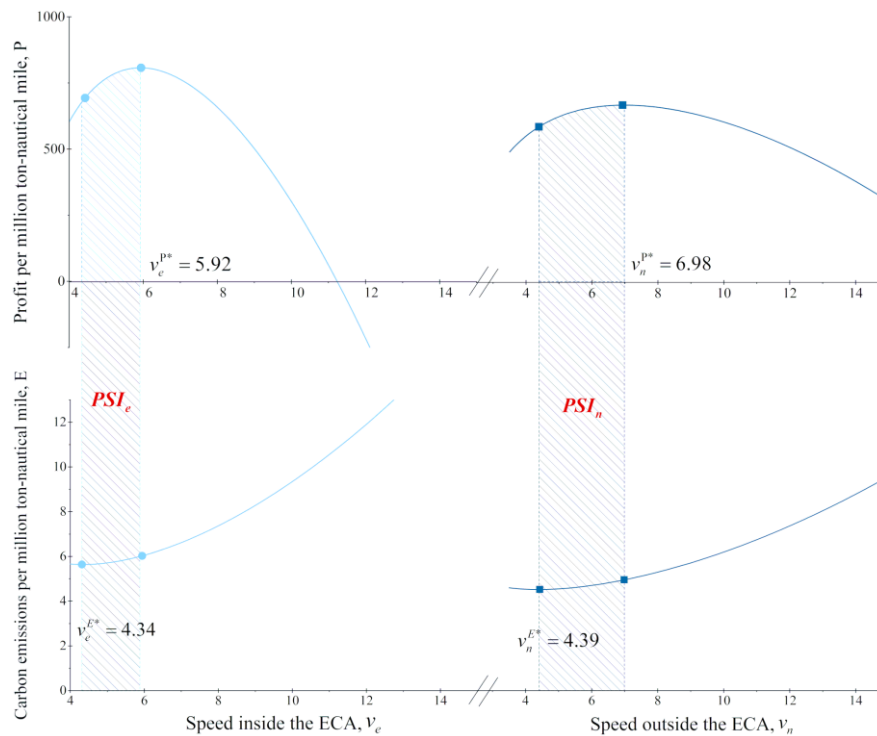


Figure 2. Profit and carbon emissions as functions of vessel speed.

It can be seen that the profit and carbon emissions improved as the speed was reduced from the design speed (V). Here, the maximal profit is regarded as the optimal profit, and the minimal carbon emissions as the optimal carbon emissions. Similarly, the speeds leading to the maximal profit and minimal carbon emissions are considered as the optimal speeds for profit and carbon emissions. Drawing on Ronen’s model [26], the two optimal speeds can be determined as follows: setting $\partial P/\partial v_e = 0$, $\partial P/\partial v_n = 0$, $\partial E/\partial v_e = 0$ and $\partial E/\partial v_n = 0$, and checking if the optimal speeds fall within allowed interval $[V, \bar{V}]$. The formulations of the optimal speeds can be simplified as:

$$v_e^{P*} = V \left(\frac{\frac{10^6}{24} C_{td} + EL^A P S^A SFOC^A P_{mgo}}{2EL^M P S^M SFOC^M (1 + \frac{W}{A})^{\frac{2}{3}} P_{mgo}} \right)^{\frac{1}{3}} \tag{18}$$

$$v_n^{P*} = V \left(\frac{\frac{10^6}{24} C_{td} + EL^A P S^A SFOC^A P_{mgo}}{2EL^M P S^M SFOC^M (1 + \frac{W}{A})^{\frac{2}{3}} P_{hfo}} \right)^{\frac{1}{3}} \tag{19}$$

$$v_e^{E*} = V \left(\frac{EL^A P S^A SFOC^A}{2EL^M P S^M SFOC^M (1 + \frac{W}{A})^{\frac{2}{3}}} \right)^{\frac{1}{3}} \tag{20}$$

$$v_n^{E*} = V \left(\frac{EL^A PS^A SFOC^A e_{mgo}}{2EL^M PS^M SFOC^M \left(1 + \frac{W}{A}\right)^{\frac{2}{3}} e_{hfo}} \right)^{\frac{1}{3}} \tag{21}$$

where v_e^{P*} and v_n^{P*} are the speeds inside and outside the ECA for the optimal profit (profit-optimum speeds), respectively; and v_e^{E*} and v_n^{E*} are the speeds inside and outside the ECA for the optimal carbon emissions, respectively (emissions-optimum speeds). According to Equations (18)–(21), v_e^{P*} , v_n^{P*} , v_e^{E*} , and v_n^{E*} are independent from X . Thus, the interval for decision-making on speed has nothing to do with the choice of X .

As indicated by Figure 2, the profit decreased and the carbon emissions increased, after the vessel speed surpassed the profit-optimum speed, and before the vessel speed reached the emissions-optimum speed. Therefore, a Pareto distribution was obtained from the shaded interval between the two optimum speeds. This interval was called the Pareto speed interval (PSI). Thus, the PSIs inside and outside the ECA can be, respectively, defined as:

$$PSI_e = [v_e^{E*}, v_e^{P*}] \tag{22}$$

$$PSI_n = [v_n^{E*}, v_n^{P*}] \tag{23}$$

The values of PSI_e and PSI_n can be calculated by Equations (18)–(21). No matter which route is selected, the speed decisions must fall within the Pareto speed intervals; that is, $v_e \in [4.34, 5.92]$ and $v_n \in [4.39, 6.98]$.

4.2.2. Route Decisions

This subsection aims to examine the effects of X on the two objectives; namely, the optimal profit and the optimal carbon emissions. As mentioned in the preceding subsection, the speed decisions should be made before route decisions, and the optimal speeds should fall within the Pareto intervals. To clarify the relationship between X and the two objectives, it is necessary to verify whether the relationship varies with the speed decisions. Therefore, six alternatives of speed decisions were designed and tested, including $v_e = 5.92$ and $v_n = 6.98$; $v_e = 5.90$ and $v_n = 6.60$; $v_e = 5.50$ and $v_n = 6.60$; $v_e = 4.50$ and $v_n = 4.55$; $v_e = 4.40$ and $v_n = 4.45$; and $v_e = 4.34$ and $v_n = 4.39$. Figure 3 displays how profit and carbon emissions per million ton-nautical-mile vary with route decisions (i.e., the distance ratio X) under the six alternatives of speed decisions.

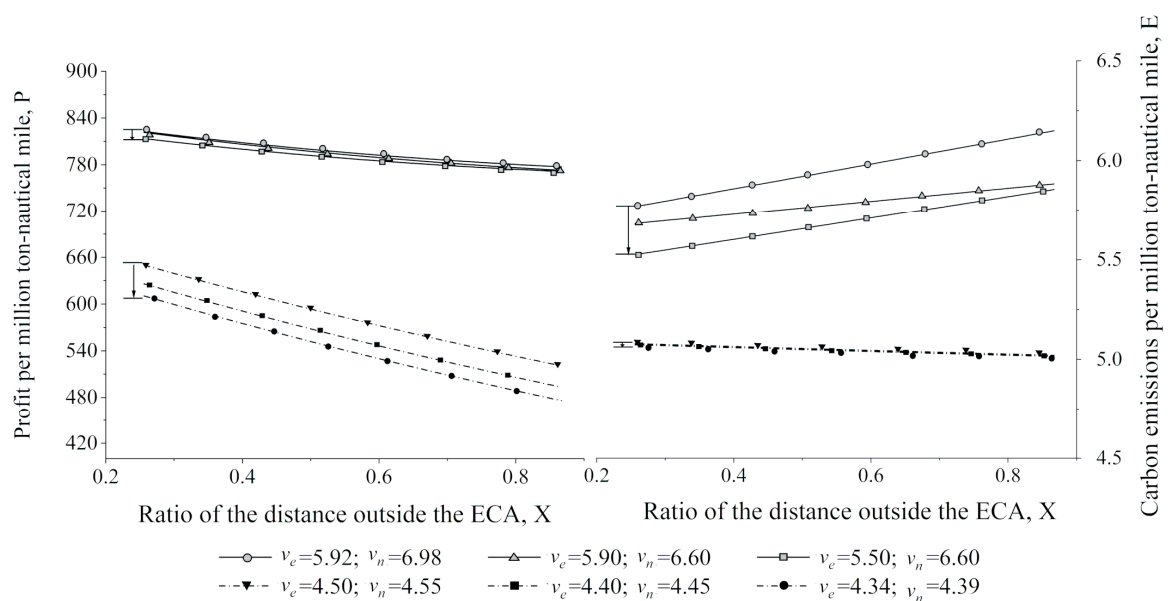


Figure 3. Profit and carbon emissions as functions of X and vessel speed.

It turns out that the value of X should be determined based on the speed decisions and the specific objective. According to the lines in the upper part of Figure 3, when the vessel speed was the profit-optimum speed ($v_e = 5.92$ and $v_n = 6.98$) or close to that speed ($v_e = 5.90$ and $v_n = 6.60$; $v_e = 5.50$ and $v_n = 6.60$), the profit declined as X increased from 0.256 to 0.867, while the carbon emissions increased linearly with the growth in X . Obviously, the operator should choose $X = 0.256$ if the speed was or close to the profit-optimum speed. The lines in the lower part shows that, when the vessel speed was the emissions-optimum speed ($v_e = 4.34$ and $v_n = 4.39$) or close to that speed ($v_e = 4.50$ and $v_n = 4.55$; $v_e = 4.40$ and $v_n = 4.45$), both profit and carbon emissions decreased with the growth in X . In this case, it is hard to make the decision about X . But, under these speed decisions, the operator can minimize the carbon emissions by setting X as 0.867.

As shown in Figure 3, both profit and carbon emissions will decrease if the operator slows down the vessel, revealing that speed reduction, also known as slow steaming, suppresses carbon emissions. It can also be observed that, if the vessel runs close to the profit-optimum speed, the speed reduction will have a greater suppression on carbon emissions and the profit decrease will not be obvious. However, if the operator blindly pursues carbon emissions through slow steaming, a fraction of carbon emissions will be reduced at the cost of a huge amount of profit.

4.2.3. Tradeoff between Profit and Carbon Emissions

The optimal profits and carbon emissions were examined under different objectives and scenarios (Figure 4). Since China designated its ECA in 2015, the HFO price and MGO price soared from 181 and 476 USD/ton to 542 and 886 USD/ton, respectively [52]. Concerns have arisen about whether the fuel prices will continue to inflate with the issuance of even stricter environmental regulations and the incoming 0.5% global sulfur cap, which may stimulate the demand for low-sulfur fuels. However, some experts argued that the fuel prices will gradually decrease, thanks to the improvement of oil refining technology.

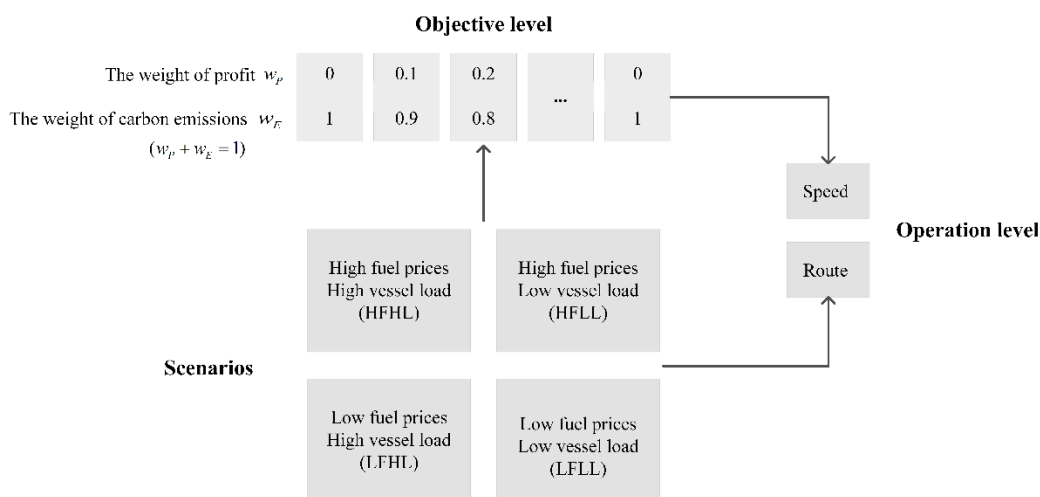


Figure 4. Different objectives and scenarios.

The related studies have shown that fuel price and load-capacity ratio of the vessel (vessel load) directly relate to profit and bunker consumption [53,54]. Following this train of thought, four scenarios were designed based on actual fuel prices and vessel loads, with the vessel load ranging between 48% and 100% [55]. The literature has shown that operators pay different levels of attention to carbon emissions, contingent on the firm size, the economic environment, and regulations [19]. As shown in Figure 4, different weights were selected from [0, 1] and assigned to the profit and carbon emissions, resulting in 10 different tradeoffs between profit and carbon emissions.

The optimal profit and carbon emissions were determined by the weighted comprehensive criterion method (WCCM) [56]. This method can normalize profit and emissions on different scales. The normalized profit and carbon emissions can be respectively expressed as:

$$P_N(v_e, v_n, X) = \frac{P^{max} - P(v_e, v_n, X)}{P^{max}} \quad (24)$$

$$E_N(v_e, v_n, X) = \frac{E(v_e, v_n, X) - E^{min}}{E^{min}} \quad (25)$$

where $P(v_e, v_n, X)$ is the original profit; P^{max} is the maximal profit; $E(v_e, v_n, X)$ is the original carbon emission value; E^{min} is the minimal carbon emission value; P_N is the decrement from the maximal profit; E_N is the increment from the minimal carbon emissions. Obviously, the profit is negatively correlated with P_N , and carbon emissions are positively correlated with E_N .

Thus, the bi-objective optimization was transformed into a single-objective problem:

$$\text{Minimize } Z(v_e, v_n, X) = w_p P_N(v_e, v_n, X) + w_E E_N(v_e, v_n, X) \quad (26)$$

where w_p and w_E are the weighting coefficients of the two objectives; namely, profit and carbon emissions ($w_p + w_E = 1$ and $w_p, w_E \geq 0$).

The Pareto frontiers in Figure 5 visualize the tradeoffs between P_N and E_N in different scenarios. The area above each frontier line represents the possible values of P_N and E_N . Of course, the operator decisions only correspond to the points on the frontier lines. It can be seen that carbon emissions surged up at the maximal profit, while the profit dropped rapidly at the minimal carbon emissions. The operator needs to strike a balance between the two conflicting objectives.

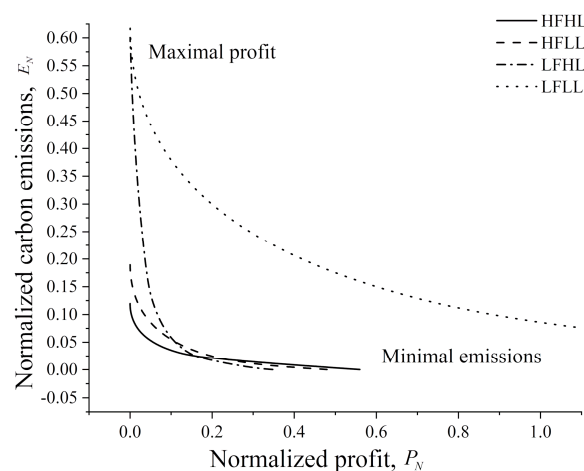


Figure 5. The Pareto frontiers of P_N and E_N .

4.3. Results and Analysis

4.3.1. Results on Normalized Profit and Carbon Emissions

Figure 6 displays the variations in P_N and E_N with the weighting coefficients of profit w_p under different scenarios. As shown in the figure, the value of P_N decreased with the growth in w_p , while the value of E_N exhibited an increasing trend. Both P_N and E_N were at a good level at the intersection of the two curves ($P_N = E_N$), which represents the most balanced tradeoff. The following results can be derived from the observations:

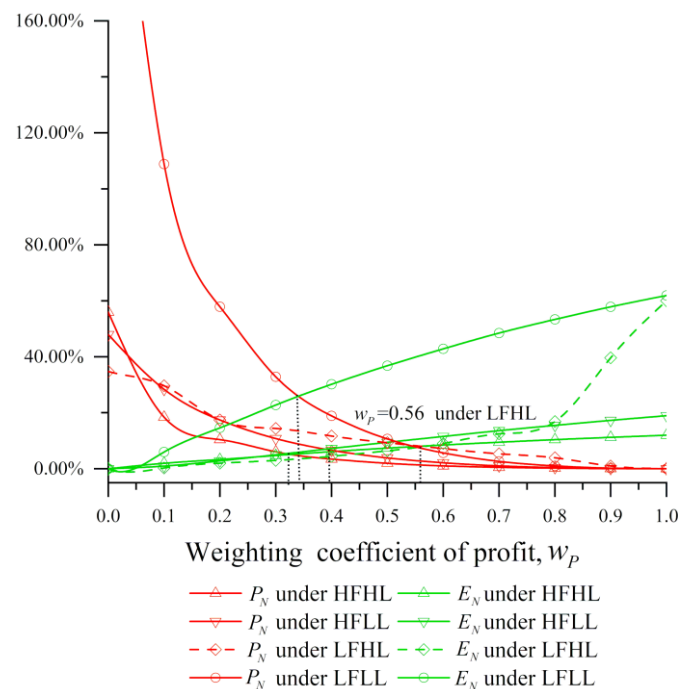


Figure 6. The values of P_N and E_N under different scenarios.

Results 1. The operator should select the w_p corresponding to $P_N = E_N$, which can be identified easily at the intersection of the two curves. Note that the w_p value is suggested rather than optimal, because the operator can still weigh between the two objectives at their discretion.

Results 2. The w_p corresponding to the most balanced tradeoff was smaller than 0.5 in all scenarios except the LFHL (Figure 6). To strike a balance between profit and carbon emissions, the operator may need to increase the value of w_p , i.e., focus more on profit, under the LFHL scenario.

Facing a high fuel price or low vessel load (e.g., under HFHL, HFLL, and LFLL), the operator may find it hard to make much profit (i.e., these scenarios are profit inefficient), and would rather devote more effort to reducing carbon emissions. If the operator still pursues profit under these profit inefficient scenarios, the carbon emissions will increase, which goes against the philosophy of sustainable operation. By contrast, if it is easy to make profit (e.g., under the profit efficient scenario of LFHL), the operator will pay more attention to profit-making, which verifies Result 2.

4.3.2. Results on Profit and Carbon Emissions

Figure 7 illustrates how profit (P) and carbon emissions (E) vary with different scenarios, respectively. It can be seen that both P and E increased with w_p . The effects of vessel load (Result 3) were derived by comparing HLs and LLs, while the effects of fuel price (Result 4) were determined by comparing HF and LF.

Result 3. With the growth in vessel load (i.e., from HFLL to HFHL, or from LFLL to LFHL), P increased and E declined, indicating that a high vessel load benefits the economy and the environment.

Result 4. The decrease of fuel price (i.e., from HFHL to LFHL, or from HFLL to LFLL) led to significant growth of P and a slight increase in E with high w_p values, but had no impact on E with low w_p values.

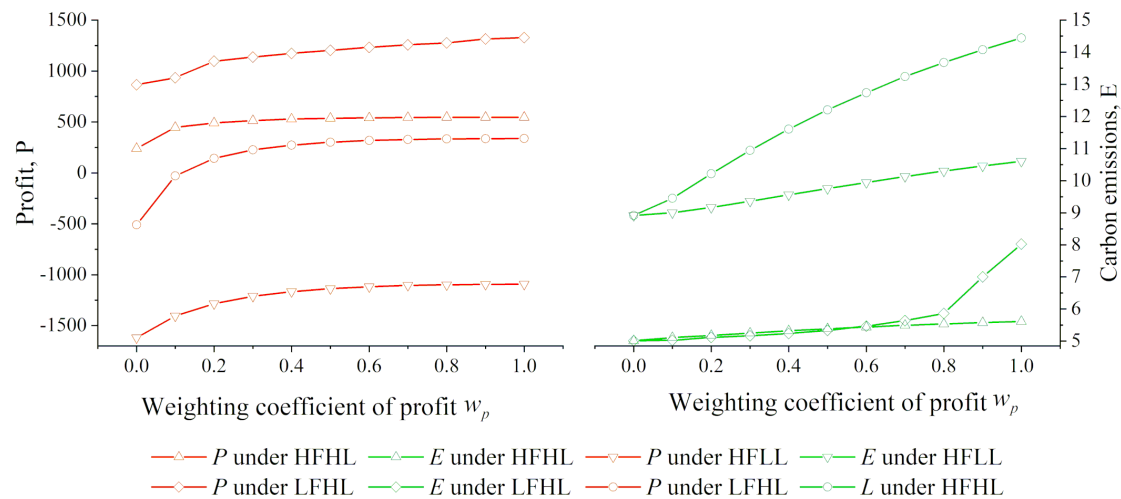


Figure 7. The profit and carbon emissions under different scenarios.

4.3.3. Decisions under Different Scenarios

Figure 8 illustrates how the decision of v_e and the decision of v_n vary with the weighting coefficients of profit w_p under different scenarios, respectively. The following results were obtained.

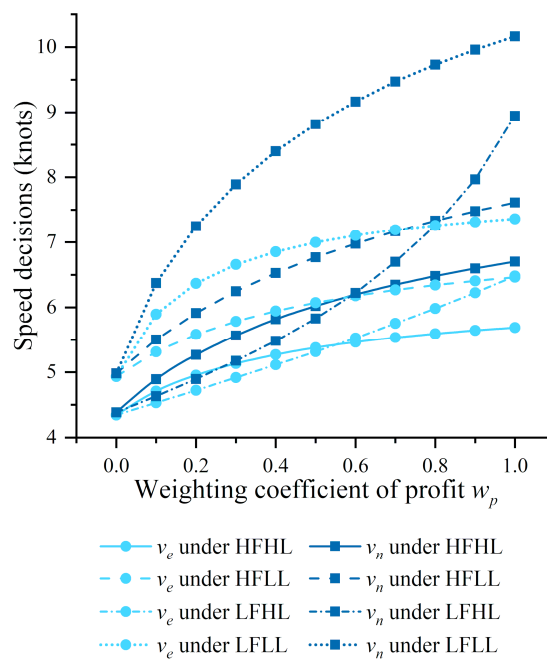


Figure 8. Speed decisions under different scenarios.

Result 5. Both v_e and v_n increased with the growth in w_p . In addition, v_e was always below v_n , but the speed difference between v_e^{E*} and v_n^{E*} (at $w_p = 0$) is negligible.

Result 6. Both v_e and v_n moved upwards at the decrease of vessel load or the fuel price. However, the fuel price exerted little impact on the speeds v_e^{E*} and v_n^{E*} at $w_p = 0$.

The above two Results indicate that the operator should increase the vessel speed under LFLL and slow down the vessel under HFHL.

Figure 9 describes the relationship between optimal distance ratio X and the weighting coefficient of profit under different scenarios. The choices of the ratio at different fuel prices and vessel loads are summed up below.

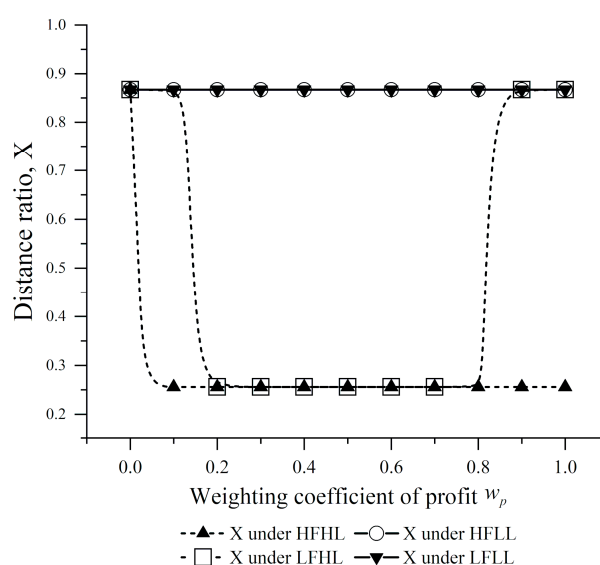


Figure 9. Route decisions under different scenarios.

Result 7. The distance ratio was optimal at 0.256 if $w_p = \{0.1, 0.2, \dots, 1.0\}$ under the HFHL or $w_p = \{0.2, 0.3, \dots, 0.8\}$ under the LFHL.

Result 8. The distance ratio was optimal at 0.867 if $w_p = 0$ under the HFHL, $w_p = \{0, 0.1\}$ or $w_p = \{0.9, 1\}$ under the LFHL, or w_p of any value under HFLF and LFLL. If the vessel load is at a low level, the operator should sail outside the ECA as much as possible.

Note that, if the operator wants to minimize the carbon emissions ($w_p = 0$), he/she must reroute and sail further outside the ECA ($X = 0.867$), regardless of the fuel price and vessel load. According to IMO [16], the MGO, which is mainly consumed inside the ECA, has a greater carbon emission factor than the HFO. In other words, compliant fuel containing less sulfur may emit more carbon. Considering the high price and high carbon emission factor of the MGO, the operator ought to sail outside the ECA as much as possible, if the vessel load is very low.

4.4. Sensitivity Analysis

4.4.1. Analysis of Vessel Size

This subsection employs our bi-objective optimization method to calculate the suggested w_p , the optimal distance ratio, and the optimal speed for vessels of different sizes. Here, the vessel size is measured by cargo capacity. The target vessels include four bulk carriers and three containerships. Table 3 lists the parameters of these vessels. Table 4 and Figures 10–16 provide the computed results. The computed results were examined to verify if Results 1–8 apply to bulk carriers and containerships of different sizes and with varied engine parameters.

Table 3. The parameters of different vessels.

Vessel Type	Cargo Capacity (dwt)	Lightship Weight (tons)	Design Speed (knots)	Main Engine Power (kW)	SFOC ^M (g/kWh)
Panamax bulker	88,291	12,000	14	12,268	172
Handymax bulker	57,025	10,900	14.2	9480	165
Handy-size bulker	33,945	8480	14.5	7135	173
	29,540	8005	14	7135	173
Neo-Panamax containership	120,445 (8530 TEU)	30,036	25	49,000	168
Intermediate containership	68,191 (5446 TEU)	24,621	24.5	43,097	166
Feeder containership	35,038 (2742 TEU)	12,725	21.5	21,770	172

Table 4 presents the suggested value of w_p for different vessels. The calculation results show that Result 1 can be extended to all target vessels: the operators can optimize and balance profit and carbon emissions using the w_p that makes $P_N = E_N$. The following can also be derived from Table 4.

Result 9. For Panamax bulker, Handymax bulker, Neo-Panamax containership, and Intermediate containership, the suggested w_p is greater than 0.5 under LFHL, and smaller than 0.5 under HFHL, HFLL, and LHLL. For Handy-size bulker and Feeder containership, the suggested w_p is smaller than 0.5 under all the scenarios.

Result 9 shows that Result 2 only applies to large vessels like Panamax bulker, Handymax bulker, Neo-Panamax containership, and Intermediate containership.

Table 4. Suggested tradeoffs for different vessels.

Vessel Type	Cargo Capacity (dwt)	Scenario	Choice of "Suggested w_p "
Panamax bulker	88,291	HFHL	0.39
		HFLL	0.29
		LFHL	0.55
		LFLL	0.46
Handymax bulker	57,025	HFHL	0.33
		HFLL	0.39
		LFHL	0.56
		LFLL	0.35
Handy-size bulker	33,945	HFHL	0.30
		HFLL	0.46
		LFHL	0.45
		LFLL	0.40
	29,540	HFHL	0.38
		HFLL	0.47
		LFHL	0.40
		LFLL	0.41
Neo-Panamax containership	120,445 (8530 TEU)	HFHL	0.43
		HFLL	0.34
		LFHL	0.58
		LFLL	0.54
Intermediate containership	68,191 (5446 TEU)	HFHL	0.41
		HFLL	0.26
		LFHL	0.56
		LFLL	0.47
Feeder containership	35,038 (2742 TEU)	HFHL	0.23
		HFLL	0.41
		LFHL	0.48
		LFLL	0.35

Figures 10 and 11 illustrate how P and E vary with w_p of different vessels, respectively. The two figures demonstrate the applicability of Results 3–4 to all the target vessels.

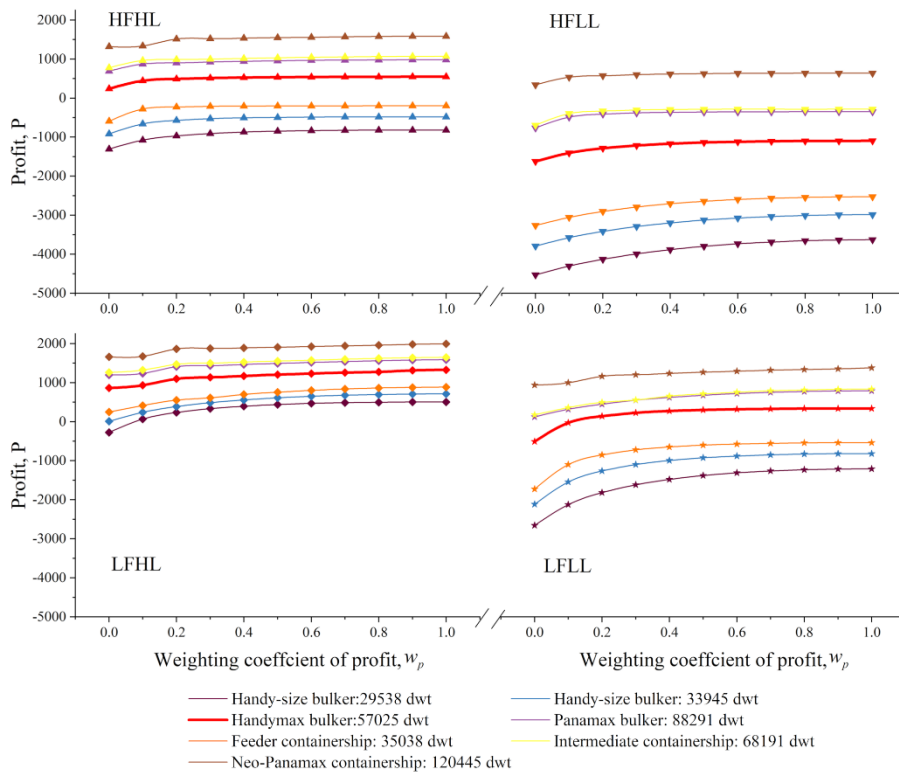


Figure 10. Profit of different vessels under different scenarios.

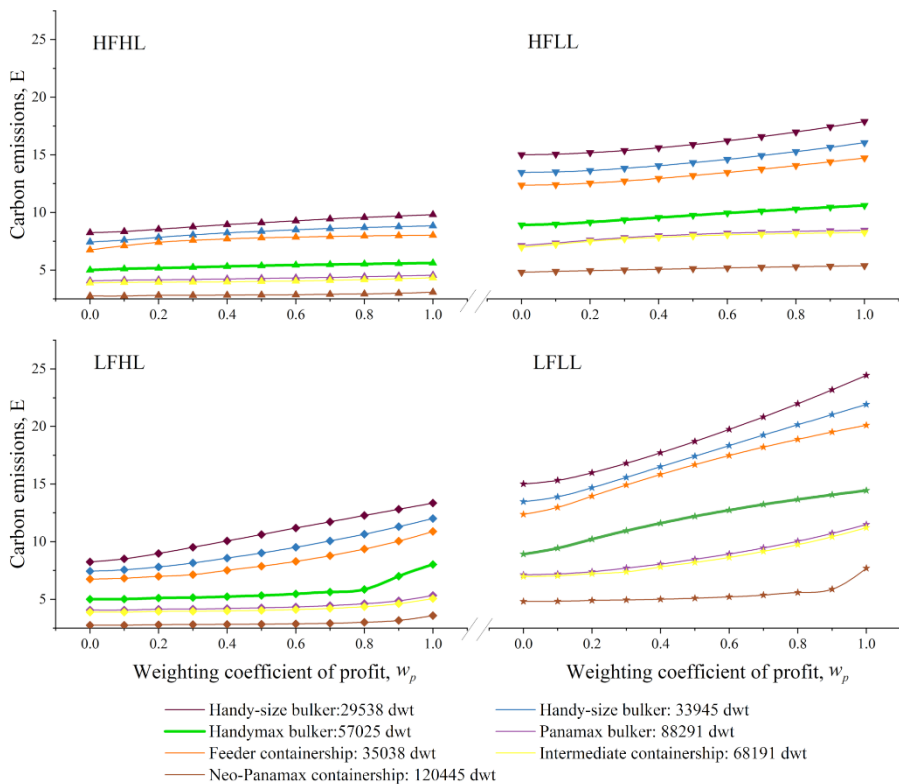


Figure 11. Carbon emissions of different vessels under different scenarios.

Figures 12 and 13 illustrate how v_e and v_n vary with w_p of different vessels, respectively. It can be seen that Result 5 applies to all the target vessels, while Result 6 is only inapplicable to the Feeder containership.

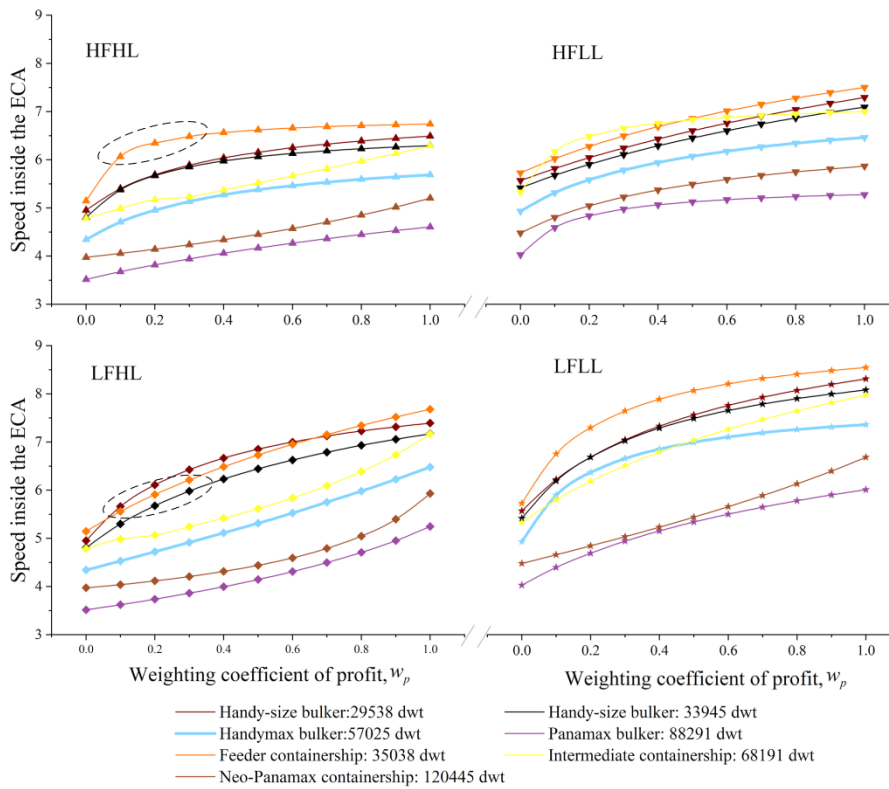


Figure 12. Speed inside the ECA of different vessels under different scenarios.

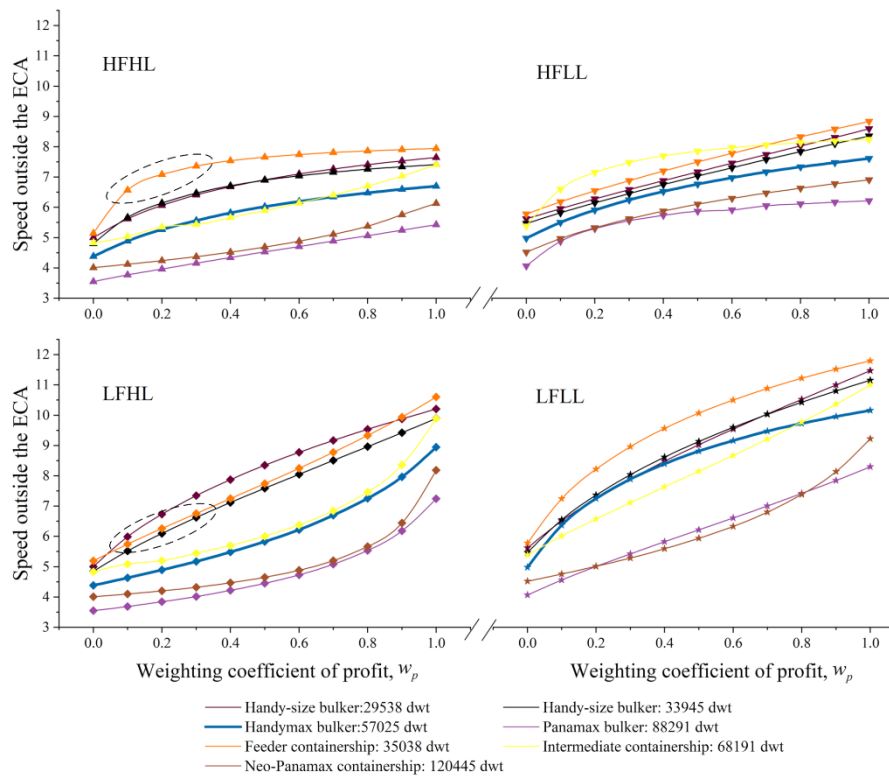
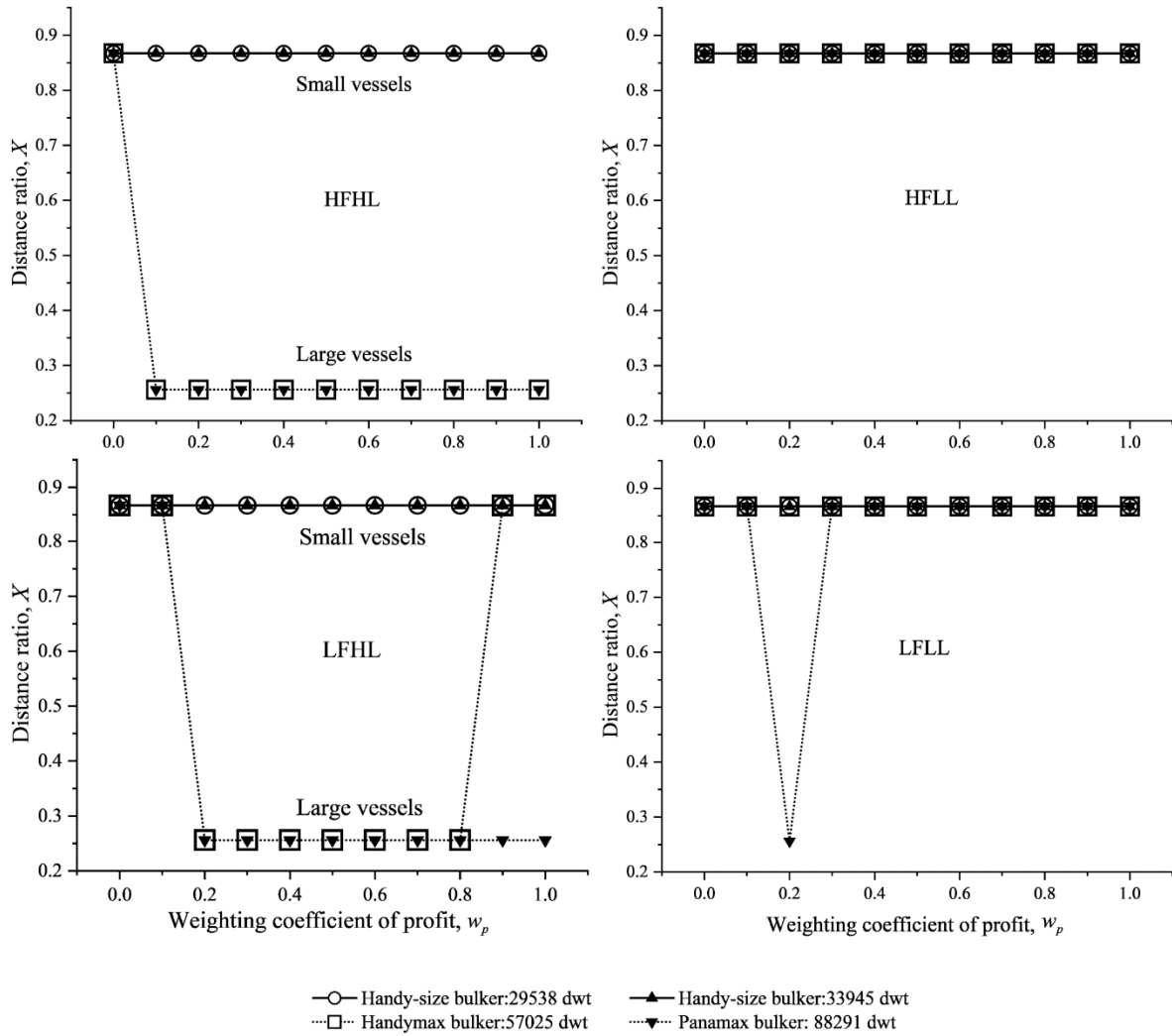


Figure 13. Speed outside the ECA of different vessels under different scenarios.

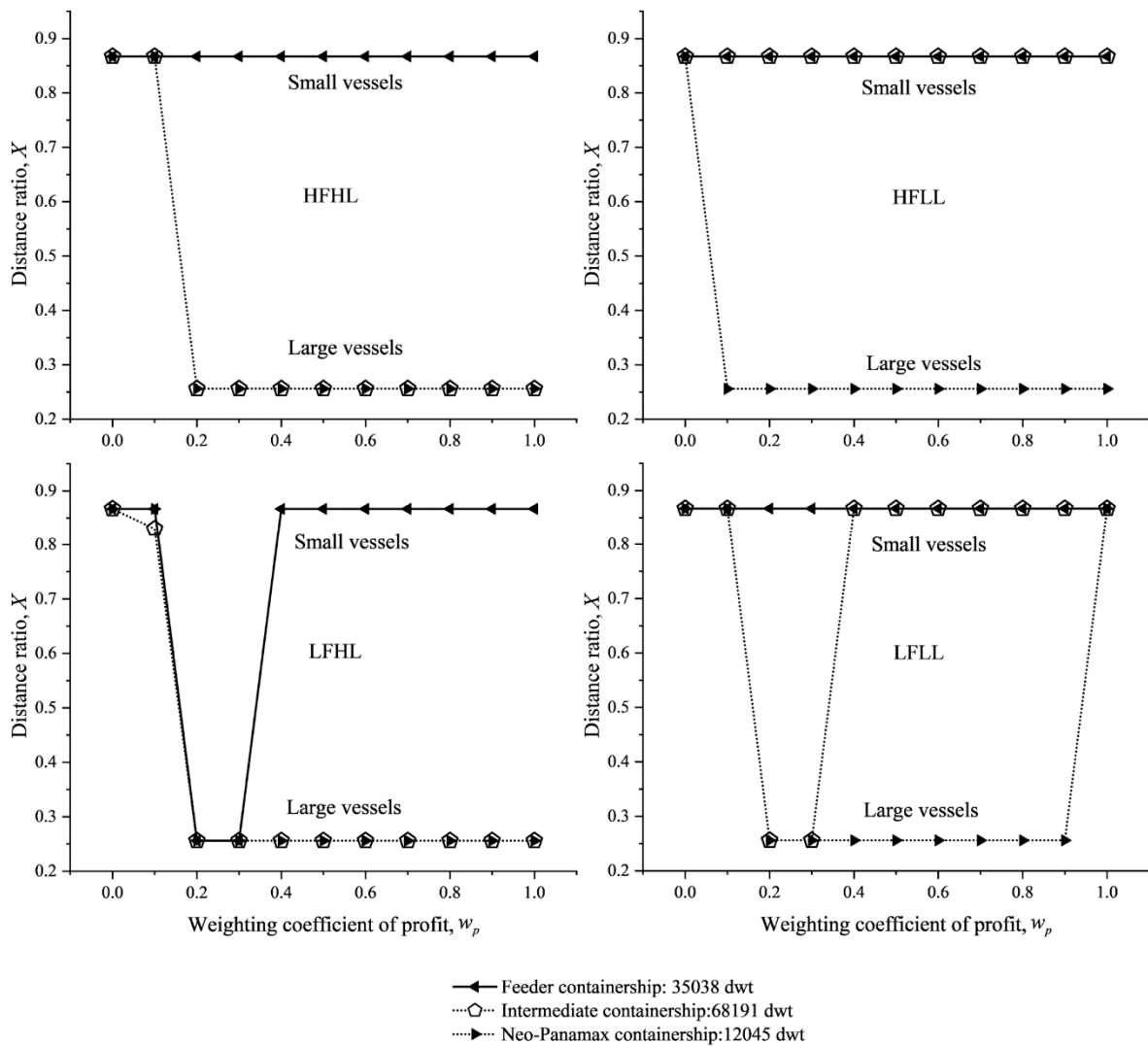
Figure 14 shows that Results 7 and 8 are valid only for Handymax bulker. Further, Result 10 was obtained regarding the relationship between X and vessel size.

Result 10. For small bulk carriers like Handy-size bulker, the route $X = 0.867$ should be selected under any scenario. For large bulk carriers like Panamax bulker, the route $X = 0.256$ should be selected if the vessel load is high. Similar rules apply to containerships: Feeder containership needs to choose $X = 0.867$ for most of the w_p values and under all the scenarios, while Neo-Panamax containership should choose $X = 0.256$. Thus, small bulk carriers and containerships should both sail further outside of the ECA.



(a) Distance ratio of different bulk carriers

Figure 14. Cont.



(b) Distance ratio of different containerships

Figure 14. Distance ratio of different vessels under different scenarios.

4.4.2. Analysis on MGO–HFO Price Spread

This subsection examines the effects of MGO–HFO price spread on speed and route. Since China designated its ECA in 2015, the MGO–HFO price spread has fluctuated between 250 USD/ton and 400 USD/ton, while the HFO price has gradually increased from 181 USD/ton to 476 USD/ton. Here, the interval of MGO–HFO price spread was set as [150, 450] USD/ton to cover the actual range in the past several years, and the HFO prices were set to 181 USD/ton, 300 USD/ton, and 476 USD/ton.

The target vessels in Section 4.1 were retained for the sensitivity analysis of MGO–HFO price spread. Figure 15 shows the optimal speeds for maximal profit ($v_e^{P^*}$ and $v_n^{P^*}$) and minimal carbon emissions ($v_e^{E^*}$ and $v_n^{E^*}$) under different MGO–HFO price spreads and HFO prices.

In Figure 15, the curves on the left show that the $v_e^{P^*}$ decreased with the growth in MGO–HFO price spread, while the curves on the right show that the $v_n^{P^*}$ increased with the price spread. The lines at the bottom remained horizontal, indicating that the $v_e^{E^*}$ and $v_n^{E^*}$ are independent of fuel price. These observations can be proven by Equations (18)–(21). On this basis, the following result can be derived.

Result 11. With the growth in MGO–HFO price spread, the Pareto speed interval inside the ECA (PSI_e) shrank, while that outside the ECA (PSI_n) widened.

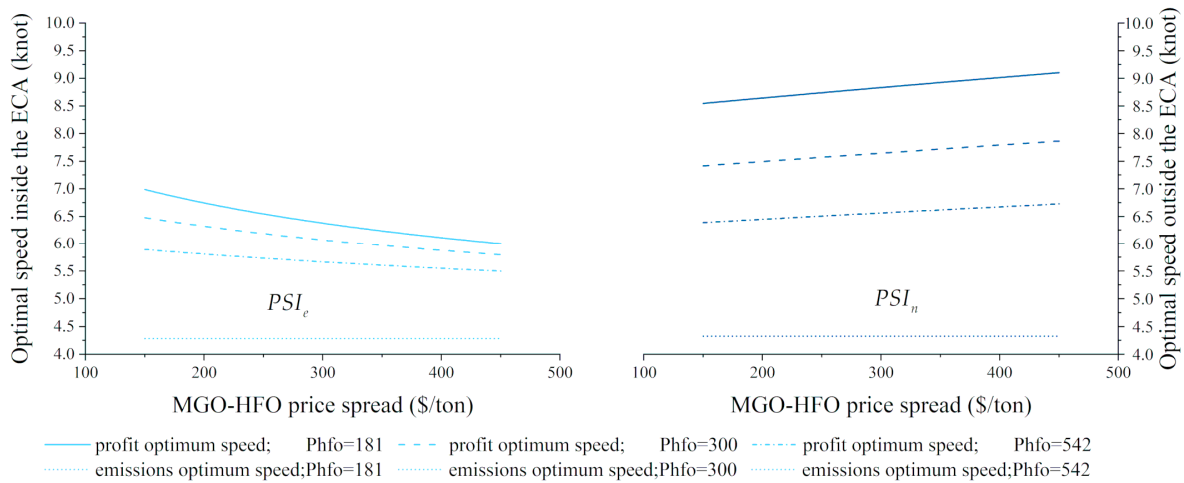
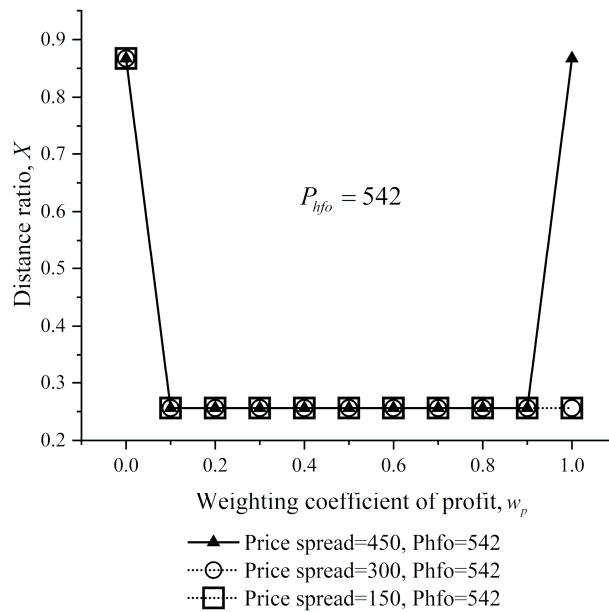


Figure 15. Optimal speed as functions of marine gas oil-heavy fuel oil (MGO-HFO) price spread.

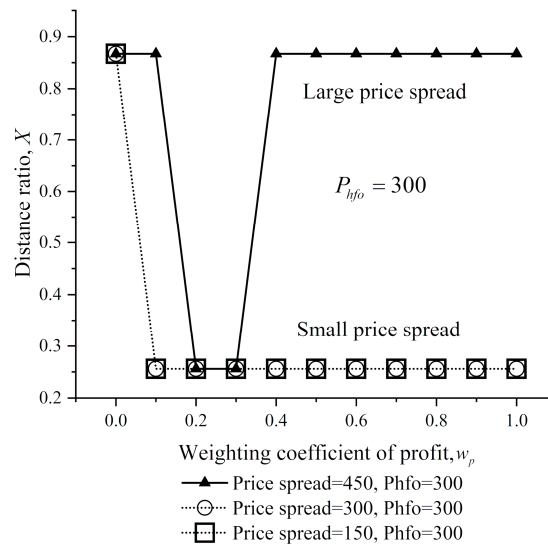
Figure 16 shows the distance ratios at different fuel prices and w_p values. The following result can be inferred from the figure.

Result 12. When the HFO prices are 181 and 300, the operator should select the route $X = 0.867$ with the increase of the MGO-HFO price spread. When the HFO price is 542, the operator should choose $X = 0.256$ for most of the w_p .

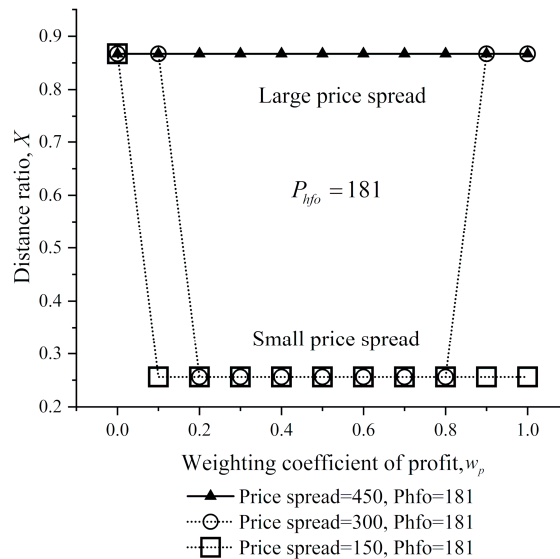


(a) Distance ratio with price of HFO constant at 542

Figure 16. Cont.



(b) Distance ratio with price of HFO constant at 300



(c) Distance ratio with price of HFO constant at 181

Figure 16. Distance ratio with different MGO–HFO price spreads and weighting coefficients.

5. Conclusions

Sustainable coastal shipping is crucial for dealing with the environmental issues derived from shipping emissions. Currently, the sustainable transformation for the coastal shipping sector is mainly reflected in two aspects; i.e., the fuel switch required by the mandatory ECA regulations, and the active adjustment of operation objectives between minimizing carbon emissions and maximizing profits. Drawing on existing models, the study formulates profit and carbon emissions for sustainable coastal shipping operations. The tradeoffs between profit and carbon emissions were investigated in detail, considering that the vessel that switches to low-sulfur fuels to sail partially inside an ECA. Firstly, the profit, carbon emissions, speed, and route were examined, revealing that all speed decisions must fall within the PSI; the speed and route decisions depend heavily on the two objectives (profit and carbon emissions); and the operator needs to strike a balance between the two conflicting objectives. Next, the optimal decisions on speed and route were investigated under different objectives, scenarios, vessel sizes, and MGO–HFO price spreads.

The results show that the operation measures and objectives depend greatly on fuel price, vessel load, and vessel parameters. The operator should speed up the vessel if he/she wants to make more profit or if the scenario is favorable for profit making; e.g., LFHL. Large vessels (e.g., Panamax bulker, Handymax bulker, Neo-Panamax containership, and Intermediate containership) should pursue more profit under the LFHL, without having to sail further outside the ECA. But this rule does not apply to small vessels like the Handy-size bulker and the Feeder containership. In addition, the increase of MGO–HFO price spread will reduce the Pareto speed interval inside the ECA, forcing the operator to slow down the vessel inside the ECA and sail further outside the ECA, especially at a low HFO price.

The research findings help operators refine their operation measures and objectives, and can be applied in the ECAs across the globe. Our method to optimize operation measures and objectives can also be extended from coastal shipping to deep-ocean shipping. In the foreseeable future, the difference of sulfur content cap between ECAs and non-ECAs will not be changed. Therefore, the research results regarding the speed difference and distance ratio between ECAs and non-ECAs will remain valid for both coastal shipping and deep-ocean shipping, as long as the vessels have to sail across the ECA. Of course, the effects of ECA regulations on coastal shipping are greater than those on deep-ocean shipping.

The main limitation of this study is that we used the fuel prices of MGO and HFO in our case study. In fact, there will be a global sulfur cap of 0.5% in 2020. In addition, the Chinese government is considering whether to carry out stricter sulfur limit of 0.1% in 2025. After 2025, the sulfur limit inside the ECA is likely to be 0.1% and the global limit outside the ECA is 0.5%. In the future, operators may use very low sulfur fuel oil (VLSFO) with 0.5% sulfur content outside the ECA and MGO inside the ECA. It would be better if we used the fuel price of MGO and VLSFO. However, as far as we know, some refiners have just started to sell VLSFO recently, and the price of VLSFO in China is still uncertain. In our opinion, the methodology in this study perhaps will still work if the operators need to switch between fuel types with different sulfur contents and different fuel prices.

Further research will explore more on how to adjust the operator's operation measures and objectives flexibly depending on regulation strictness and market situation, and probe into other abatement options like retrofitting scrubbers and investing on abatement technologies.

Author Contributions: Y.Z. and H.K. conceived the study, and were responsible for the design and development of the case study. Y.F. and J.Z. were responsible for data collection and analysis. Y.F. was also responsible for data interpretation. In addition, Y.Z. wrote the first draft of this paper.

Funding: This work was supported by the National Natural Science Foundation of China (grant number 71403035, 71902016, 71831002), the Foundation for Humanities and Social Sciences of the Ministry of Education of China (grant number 18YJC630261), the Key R&D Program for Soft Science Projects of Liaoning Province, China (grant number 2018401030), the Program for Innovative Research Team in Universities of the Ministry of Education of China (grant number IRT_17R13), and the Fundamental Research Funds for the Central Universities of China (grant numbers 3132018301 and 3132018304).

Acknowledgments: Our special thanks go to the anonymous reviewers for their constructive comments.

Conflicts of Interest: The authors declare no conflict of interest.

References

1. Yang, H.; Ma, X. Uncovering CO₂ emissions patterns from China-oriented international maritime transport: Decomposition and decoupling Analysis. *Sustainability* **2019**, *11*, 2826. [[CrossRef](#)]
2. Svindland, M. The environmental effects of emission control area regulations on short sea shipping in Northern Europe: The case of container feeder vessels. *Transp. Res. Part D Transp. Environ.* **2018**, *61*, 423–430. [[CrossRef](#)]
3. Perakis, A.N.; Denisis, A. A survey of short sea shipping and its prospects in the USA. *Marit. Policy Manag.* **2008**, *35*, 591–614. [[CrossRef](#)]
4. Cullinane, K.; Bergqvist, R. Emission control areas and their impact on maritime transport. *Transp. Res. Part D Transp. Environ.* **2014**, *28*, 1–5. [[CrossRef](#)]

5. Hilmola, O.-P. Shipping sulphur regulation, freight transportation prices and diesel markets in the Baltic Sea region. *Int. J. Energy Sect. Manag.* **2015**, *9*, 120–132. [CrossRef]
6. Gu, Y.; Wallace, S.W. Scrubber: A potentially overestimated compliance method for the emission control areas. *Transp. Res. Part D Transp. Environ.* **2017**, *55*, 51–66. [CrossRef]
7. Psaraftis, H.N.; Kontovas, C.A. Ship emissions: Logistics and other tradeoffs. In Proceedings of the 10th International Marine Design Conference (IMDC), Trondheim, Norway, 26–29 May 2009.
8. Suárez-Alemán, A.; Trujillo, L.; Medda, F. Short sea shipping as intermodal competitor: A theoretical analysis of European transport policies. *Marit. Policy Manag.* **2015**, *42*, 317–334. [CrossRef]
9. Fagerholt, K.; Gausel, N.T.; Rakke, J.G.; Psaraftis, H.N. Maritime routing and speed optimization with emission control areas. *Transp. Res. Part C Emerg. Technol.* **2015**, *52*, 57–73. [CrossRef]
10. Christodoulou, A.; Woxenius, J. Sustainable short sea shipping. *Sustainability* **2019**, *11*, 2847. [CrossRef]
11. Maersk. 2018 Sustainability Report. Available online: https://www.maersk.com/-/media/ml/about/sustainability/sustainability-new/files/apmm_sustainability_report_2018_a4_190228.pdf (accessed on 21 February 2019).
12. Stalmokaitė, I.; Yliskylä-Peuralahti, J. Sustainability transitions in Baltic Sea shipping: Exploring the responses of firms to regulatory changes. *Sustainability* **2019**, *11*, 1916. [CrossRef]
13. Jemai, J.; Zekri, M.; Mellouli, K. An NSGA-II algorithm for the green vehicle routing problem. In Proceedings of the European Conference on Evolutionary Computation in Combinatorial Optimization, Málaga, Spain, 11–13 April 2012; pp. 37–48. [CrossRef]
14. Lindstad, H.; Asbjørnslett, B.E.; Strømman, A.H. Reductions in greenhouse gas emissions and cost by shipping at lower speed. *Energy Policy* **2011**, *39*, 3456–3464. [CrossRef]
15. Lindstad, H.; Asbjørnslett, B.E.; Strømman, A.H. The importance of economies of scale for reductions in greenhouse gas emissions from shipping. *Energy Policy* **2012**, *46*, 386–398. [CrossRef]
16. International Maritime Organization (IMO). *Third IMO GHG Study 2014*; Smith, T.W.P., Jalkanen, J.P., Anderson, B.A., Corbett, J.J., Faber, J., Hanayama, S., O’Keeffe, E., Parker, S., Johansson, L., Aldous, L., et al., Eds.; International Maritime Organization (IMO): London, UK, 2014.
17. Sarkis, J. *Greening the Supply Chain*; Springer: London, UK, 2006. [CrossRef]
18. Yuen, K.F.; Thai, V.V.; Wong, Y.D. The effect of continuous improvement capacity on the relationship between corporate social performance and business performance in maritime transport in Singapore. *Transp. Res. Part E Logist. Transp. Rev.* **2016**, *95*, 62–75. [CrossRef]
19. Berg, R.V.D.; Langen, P.W.D. Environmental sustainability in container transport: The attitudes of shippers and forwarders. *Int. J. Logist. Res. Appl.* **2017**, *20*, 146–162. [CrossRef]
20. Kontovas, C.A.; Psaraftis, H.N. Reduction of emissions along the maritime intermodal container chain: Operational models and policies. *Marit. Policy Manag.* **2011**, *38*, 451–469. [CrossRef]
21. Dulebenets, M.A. The green vessel scheduling problem with transit time requirements in a liner shipping route with emission control areas. *Alex. Eng. J.* **2018**, *57*, 331–342. [CrossRef]
22. Perera, L.P.; Mo, B. Emission control based energy efficiency measures in ship operations. *Appl. Ocean Res.* **2016**, *60*, 29–46. [CrossRef]
23. Fan, L.; Huang, L. Analysis of the incentive for slow steaming in Chinese sulfur emission control areas. *Transp. Res. Rec.* **2019**, *2673*, 165–175. [CrossRef]
24. Zis, T.; Psaraftis, H.N. Operational measures to mitigate and reverse the potential modal shifts due to environmental legislation. *Marit. Policy Manag.* **2018**, *46*, 117–132. [CrossRef]
25. Fagerholt, K.; Psaraftis, H.N. On two speed optimization problems for ships that sail in and out of emission control areas. *Transp. Res. D Transp. Environ.* **2015**, *39*, 56–64. [CrossRef]
26. Ronen, D. The effect of oil price on the optimal speed of ships. *J. Oper. Res. Soc.* **1982**, *33*, 1035–1040. [CrossRef]
27. Doudnikoff, M.; Lascoste, R. Effect of a speed reduction of containerships in response to high energy costs in sulphur emission control areas. *Transp. Res. D Transp. Environ.* **2014**, *28*, 51–61. [CrossRef]
28. Zis, T.; North, R.J.; Angeloudis, P.; Ochieng, W.Y. Environmental balance of shipping emissions reduction strategies. *Transp. Res. Rec.* **2015**, *2479*, 25–33. [CrossRef]
29. Adland, R.; Fonnes, G.; Jia, H.; Lampe, O.D.; Strandenes, S.P. The impact of regional environmental regulations on empirical vessel speeds. *Transp. Res. D Transp. Environ.* **2017**, *53*, 37–49. [CrossRef]
30. Zhen, L.; Li, M.; Hu, Z.; Lv, W.; Zhao, X. The effects of emission control area regulations on cruise shipping. *Transp. Res. D Transp. Environ.* **2018**, *62*, 47–63. [CrossRef]

31. Chen, L.; Yip, T.L.; Mou, J. Provision of Emission Control Area and the impact on shipping route choice and ship emissions. *Transp. Res. Part D Transp. Environ.* **2018**, *58*, 280–291. [CrossRef]
32. Patricksson, Ø.; Erikstad, S.O. A two-stage optimization approach for sulphur emission regulation compliance. *Marit. Policy Manag.* **2017**, *44*, 94–111. [CrossRef]
33. Bergqvist, R.; Turesson, M.; Weddmark, A. Sulphur emission control areas and transport strategies—the case of Sweden and the forest industry. *Eur. Transp. Res. Rev.* **2015**, *7*, 10. [CrossRef]
34. Zis, T.; Psaraftis, H.N. The implications of the new sulphur limits on the European Ro-Ro sector. *Transp. Res. D Transp. Environ.* **2017**, *52*, 185–201. [CrossRef]
35. Guo, Z.; Zhang, D.; Liu, H.; He, Z.; Shi, L. Green transportation scheduling with pickup time and transport mode selections using a novel multi-objective memetic optimization approach. *Transp. Res. D Transp. Environ.* **2018**, *60*, 137–152. [CrossRef]
36. Corbett, J.; Wang, H.; Winebrake, J. The effectiveness and costs of speed reductions on emissions from international shipping. *Transp. Res. D Transp. Environ.* **2009**, *14*, 593–598. [CrossRef]
37. Kim, J.-G.; Kim, H.-J.; Lee, P.T.-W. Optimising containership speed and fleet size under a carbon tax and an emission trading scheme. *Int. J. Shipp. Trans. Logist.* **2013**, *5*, 571–590. [CrossRef]
38. Wen, M.; Pacino, D.; Kontovas, C.A.; Psaraftis, H.N. A multiple ship routing and speed optimization problem under time, cost and environmental objectives. *Transp. Res. D Transp. Environ.* **2017**, *52*, 303–321. [CrossRef]
39. Psaraftis, H.N.; Kontovas, C.A. Balancing the economic and environmental performance of maritime transportation. *Transp. Res. D Transp. Environ.* **2010**, *15*, 458–462. [CrossRef]
40. Wong, E.; Tai, A.; Lau, H.; Raman, M. An utility-based decision support sustainability model in slow steaming maritime operations. *Transp. Res. Part E Logist. Transp. Rev.* **2015**, *78*, 57–69. [CrossRef]
41. Cheaitou, A.; Cariou, P. Greening of maritime transportation: A multi-objective optimization approach. *Ann. Oper. Res.* **2019**, *273*, 501–525. [CrossRef]
42. Mansouri, S.A.; Lee, H.; Aluko, O. Multi-objective decision support to enhance environmental sustainability in maritime shipping: A review and future directions. *Transp. Res. Part E Logist. Transp. Rev.* **2015**, *78*, 3–18. [CrossRef]
43. Barrass, C.B. *Ship Design and Performance for Masters and Mates*; Butterworth-Heinemann: Oxford, UK, 2004; pp. 228–234. [CrossRef]
44. Psaraftis, H.N.; Kontovas, C.A. Speed models for energy-efficient maritime transportation: A taxonomy and survey. *Transp. Res. C Emerg. Technol.* **2013**, *26*, 331–351. [CrossRef]
45. Koza, D.F. Liner shipping service scheduling and cargo allocation. *Eur. J. Oper. Res.* **2019**, *275*, 897–915. [CrossRef]
46. Wang, S.; Meng, Q. Sailing speed optimization for container ships in a liner shipping network. *Transp. Res. Part E Logist. Transp. Rev.* **2012**, *48*, 701–714. [CrossRef]
47. Cariou, P.; Cheaitou, A. The effectiveness of a European speed limit versus an international bunker-levy to reduce CO₂ emissions from container shipping. *Transp. Res. D Transp. Environ.* **2012**, *17*, 116–123. [CrossRef]
48. Trawind Shipping Logistics. Available online: http://www.trawind.com/en/index.php?p=global_shipping&lanmu=13&f_id=26&c_id=68 (accessed on 24 January 2019).
49. Bunkerworld, Bunker Prices in Shanghai. Available online: www.bunkerworld.com/prices/ (accessed on 20 December 2018).
50. Portdalian. Available online: <http://www.dlport.cn/> (accessed on 20 December 2018).
51. Portguangzhou. Available online: <http://www.gzpgroup.com/> (accessed on 20 December 2018).
52. Clarksons. Available online: <https://sin.clarksons.net/Timeseries/Advanced> (accessed on 12 January 2019).
53. Sheng, D.; Meng, Q.; Li, Z. Optimal vessel speed and fleet size for industrial shipping services under the emission control area regulation. *Transp. Res. C Emerg. Technol.* **2019**, *105*, 37–53. [CrossRef]
54. Psaraftis, H.N.; Kontovas, C.A. Ship speed optimization—concepts, models and combined speed-routing scenarios. *Transp. Res. C Emerg. Technol.* **2014**, *44*, 52–69. [CrossRef]
55. Shipxy. Available online: <http://report.shipxy.com/rtv/home.html?flag=3> (accessed on 24 January 2019).
56. Caramia, M.; Dell’Olmo, P. *Multi-Objective Management in Freight Logistics: Increasing Capacity, Service Level and Safety with Optimization Algorithms*; Springer: New York, NY, USA, 2008. [CrossRef]

